

# Structural Studies of Copper-Exchanged A Zeolites by Electron Spin Echo Spectrometry: Adsorbate Interactions

Tsuneki Ichikawa<sup>†</sup> and Larry Kevan<sup>\*</sup>

Contribution from the Faculty of Engineering, Hokkaido University, Sapporo 060, Japan, and the Department of Chemistry, University of Houston, Houston, Texas 77004.

Received February 2, 1981

**Abstract:** Electron spin echo signals of dehydrated copper-exchanged zeolites have been obtained which suggest that the cupric ions initially located in site S2 in the center of hexagonal faces between the  $\alpha$  and  $\beta$  cages in the hydrated zeolite migrate  $\sim 0.12$  nm along the axis of a hexagonal face in the  $\beta$  cage upon dehydration. In site S2' the cupric ions interact more weakly with Al nuclei in the hexagonal face. The cupric ions return to site S2 upon rehydration, where they are coordinated to two water molecules; one water is in the  $\beta$  cage and the other is in the  $\alpha$  cage. The cupric ions also move back close to site S2 when methanol is the adsorbate, but they are then coordinated to only one methanol molecule located in the  $\alpha$  cage. The cupric ions only slightly change their position from site S2' upon the adsorption of nonpolar ethylene molecules; they are weakly coordinated to one ethylene molecule in the  $\alpha$  cage. The change of the ESR spectra observed upon dehydration and upon subsequent molecular adsorption can also be correlated with the migration of cupric ions between sites S2' and S2.

Zeolites are among the most important catalysts for a wide variety of chemical reactions. The advantage of using zeolites as catalysts is that their catalytic activity can be controlled by cation exchange within the aluminosilicate structure. Since the catalytic properties of cation-exchanged zeolites are strongly dependent on the nature and location of the cations,<sup>1</sup> it is important to elucidate the location of the cations and the number and orientation of the molecules coordinated to them. Electron spin resonance (ESR) spectroscopy has been widely used for the characterization of cations having unpaired electrons.<sup>2-13</sup> The resultant spectra have been used to interpret the atomic and the molecular environment of paramagnetic cations. Copper-exchanged zeolites have been extensively studied<sup>3-13</sup> because this  $d^9$  ion can be conveniently studied by ESR. Several ESR spectra have been detected upon hydration, dehydration, and the adsorption of various molecules. These spectra have been indirectly assigned to the cations in different surroundings inside the zeolite framework with different coordination and symmetry of the adsorbed molecules. However, these studies have not generally given direct information about the atomic and molecular environment for the cations. Such information is contained in the superhyperfine interaction with nearby magnetic nuclei, which is too weak to be observed in a conventional ESR experiment.

We have recently shown that electron spin echo (ESE) spectrometry is quite useful for elucidating the local structure of paramagnetic species in catalytic solids.<sup>14-18</sup> The main advantage of this method is directly related to the types, number, and distances of magnetic nuclei surrounding the paramagnetic species. Using this method, we have found that cupric ions in doped, hydrated A zeolites are located in the center of a hexagonal face or 6-ring between the  $\alpha$  and  $\beta$  cages, and are coordinated to two water molecules.<sup>18</sup>

In the present work the technique of ESE spectrometry is applied to the study of the cupric ion location in dehydrated zeolites and the geometric structure of additionally adsorbed molecules near the cupric ions. This also allows us to relate the observed ESR spectra to the location of the cations.

## Experimental Section

Partially copper(II)-exchanged A zeolites were prepared from Linde 3-A (K-A), 4-A (Na-A), and 5-A (Ca-A) powdered zeolites. The extent of cation exchange by cupric ions was estimated to be less than 0.28%. These samples were dried at 350 K for 24 h, sealed in 3 mm o.d. suprasil quartz tubes, heated in vacuo up to 673 K at increasing temperatures for intervals of 1 h, oxidized at 673 K for 1 h under an oxygen pressure of 760 torr, and then heated for 15 h at the same temperature in vacuo ( $10^{-4}$  torr). The process of heating at a given temperature in

vacuo is commonly called "activation" in the catalysis literature.

Methanol (Merck spectroscopic grade) and deuterated compounds  $D_2O$ ,  $CD_3OH$ ,  $CH_3OD$ , and  $C_2D_4$  (99% D, Stohler Isotope Chemicals) were used without further purification. These molecules, except  $C_2D_4$ , were adsorbed by exposing the saturation vapor pressure of the molecules to the activated sample in 20 torr portions at room temperature.

ESR spectra were obtained at 77 K on a Varian E-4 spectrometer. ESE signals were obtained at 4.2 K on a home-built spectrometer with 1 kW maximum microwave pulses.<sup>19</sup> The pulses used had a width of 30 ns, a power of  $\sim 100$  W, and a frequency of 9.15 GHz. Unless otherwise stated, the magnetic field and the microwave frequency were fixed at 315 mT and 9.15 GHz, respectively, conditions at which the ESE signals show the maximum intensity. The two-pulse ESE method was used for observing the nuclear modulation from  $^{27}Al$  nuclei, whereas the three pulse ESE method was applied for the observation of deuteron nuclear modulation. In the three-pulse ESE experiment the time interval between the first and the second pulse was fixed at 0.26  $\mu s$ , which was effective for observing the nuclear modulation from deuterons without interference from  $^{27}Al$  nuclei.

## Theory

In a two-pulse electron spin echo experiment  $90^\circ$  and  $180^\circ$  pulses separated by a time interval  $\tau$  are applied to the spin system and the echo is observed at time  $\tau$  after the second pulse. In a three-pulse experiment, two  $90^\circ$  pulses separated by time  $\tau$  are followed by a time  $T$  after which a third  $90^\circ$  pulse is applied which stimulates an echo produced  $\tau$  after the third pulse. The echo decay envelope is often modulated by interaction with surrounding nuclei, the theory of which has been extensively described.<sup>20-22</sup>

(1) Smith, J. V. In "Zeolite Chemistry and Catalysis", Rabo, J. A., Ed.; American Chemical Society: Washington, D.C., 1976; Chapter 1.

(2) Herman, R. G.; Flentge, D. R. *J. Phys. Chem.* **1978**, *82*, 720 and ref 2-22 in this paper.

(3) Tikhomirova, N. N.; Nikolaeva, I. V. *Zh. Strukt. Khim.* **1969**, *10*, 547 and references therein.

(4) Leith, I. R.; Leach, H. F. *Proc. R. Soc. London, Ser. A* **1972**, *A330*, 247.

(5) Conesa, J. C.; Soria, J. J. *J. Chem. Soc., Faraday Trans. 1* **1978**, *74*, 406.

(6) Conesa, J. C.; Soria, J. J. *J. Chem. Soc., Faraday Trans. 1* **1978**, *74*, 423.

(7) Conesa, J. C.; Soria, J. J. *J. Phys. Chem.* **1978**, *82*, 1575; **1978**, *82*, 1575.

(8) Conesa, J. C.; Soria, J. J. *J. Phys. Chem.* **1978**, *82*, 1847.

(9) Conesa, J. C.; Soria, J. J. *Magn. Reson.* **1979**, *33*, 295.

(10) Horser, H.; Primet, M.; Vadrine, J. C. *J. Chem. Soc., Faraday Trans. 1* **1978**, *74*, 335.

(11) Iton, L. E.; Turkevich, J. *J. Phys. Chem.* **1977**, *81*, 435.

(12) Kasai, P. H.; Bishop, R. J. *J. Phys. Chem.* **1978**, *82*, 279.

(13) Herman, R. G. *Inorg. Chem.* **1980**, *18*, 995.

(14) Ichikawa, T.; Kevan, L. *J. Am. Chem. Soc.* **1980**, *102*, 2650.

(15) Narayana, M.; Kevan, L. *J. Am. Chem. Soc.* **1981**, *103*, 1618.

(16) Narayana, M.; Li, A. S. W.; Kevan, L. *J. Phys. Chem.* **1981**, *85*, 132.

(17) Dikanov, S. A.; Yudanov, V. F.; Samoilov, R. I.; Tsvetkov, Yu. D. *Chem. Phys. Lett.* **1977**, *52*, 520.

(18) Ichikawa, T.; Kevan, L. *J. Chem. Soc., Faraday Trans. 1*, in press.

(19) Ichikawa, T.; Kevan, L.; Narayana, P. A. *J. Phys. Chem.* **1979**, *83*,

3378.

(20) Mims, W. B. *Phys. Rev.* **1972**, *B5*, 2409.

\* University of Houston.

<sup>†</sup> Hokkaido University.

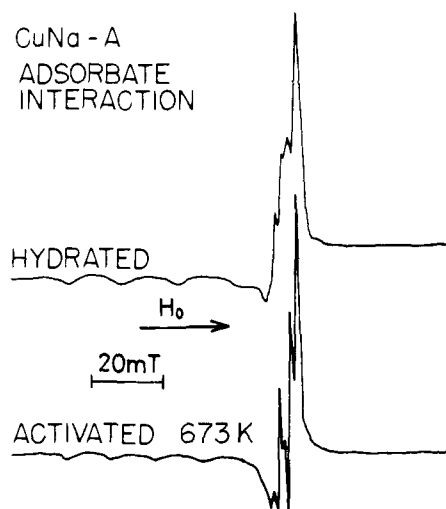


**Figure 1.** ESR spectra of  $\text{Cu}^{2+}$  in hydrated (upper) and dehydrated or activated (lower) Na-A zeolite.

The data reduction method involving a ratio analysis procedure has been described in detail.<sup>22</sup> From a comparison of theoretical and experimental ratios, the number of nuclei contributing to the modulation pattern,  $n$ , their distance to the paramagnetic center,  $r$ , and the isotropic hyperfine coupling,  $a_{\text{iso}}$ , can be determined. The parameter  $n$  is constrained to be integral and can typically be uniquely determined up to about  $n = 10$ . For larger values of  $n$  the uncertainty is about 10%. The parameter  $r$  can normally be determined to  $\pm 0.01$  nm, and  $a_{\text{iso}}$  to  $\pm 15\%$  for good quality data. The simulated modulation patterns are directly compared with the experimental curves by using a general decay function of the type

$$g(T) = \exp(A_0 + A_1 T + A_2 T^2 + A_3 T^3) \quad (1)$$

for three-pulse echo data where the coefficients are determined by a least-squares method.<sup>22</sup>

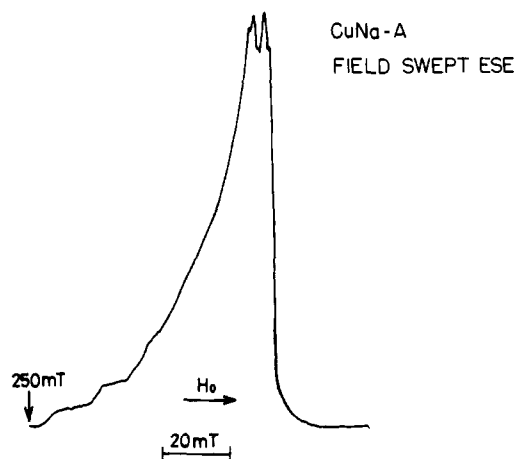
### Results

Figure 1 compares the ESR spectrum of the "activated" or dehydrated CuNa-A zeolite with that of a hydrated sample.<sup>18</sup> The spectra of the other activated zeolites (CuK-A and CuCa-A) were similar. The activation resulted in the development of sharply defined hyperfine splittings in the  $g$  region.

The magnetic field dependence of the ESE intensity for the activated zeolite is shown in Figure 2. The spectral shape was the same as the first integral of the ESR spectrum. This certifies that all  $\text{Cu}^{2+}$  detected by ESR give an ESE signal.

The two-pulse ESE signal for the activated CuNa-A zeolite is shown in Figure 3 with that of the hydrated zeolite. The signals for the other zeolites are similar. The echo signal is modulated with a frequency close to the free nuclear precession frequency of  $^{27}\text{Al}$  which is 3.5 MHz in a 315 mT field. The  $^{23}\text{Na}$  modulation frequency is close to that of  $^{27}\text{Al}$  and could contribute to the modulation. However, since the CuK-A and CuCa-A zeolites give the same modulation pattern, all the observed modulation is assigned to  $^{27}\text{Al}$  nuclei. It can be seen that the activated zeolite gives a much shallower modulation than does the hydrated zeolite. This suggests that the  $\text{Cu}^{2+}$  to Al distance increases on dehydration. Due to the unknown size of the  $^{27}\text{Al}$  quadrupole interaction, only a semiquantitative analysis can be done.<sup>21</sup> The modulation in the hydrated zeolite is consistent with 3 Al nuclei at a distance of  $\sim 0.3$  nm with an assumed quadrupole interaction of 0.5–1 MHz.

The ESR spectra and the modulation patterns for rehydrated zeolites were the same as those for the initial hydrated zeolites. The three-pulse electron spin echo signals for the zeolites re-



**Figure 2.** Field dependence of the two-pulse electron spin echo signal for  $\text{Cu}^{2+}$  in activated Na-A zeolite. Time separation of the two pulses is fixed at  $\tau = 0.26$   $\mu\text{s}$ .

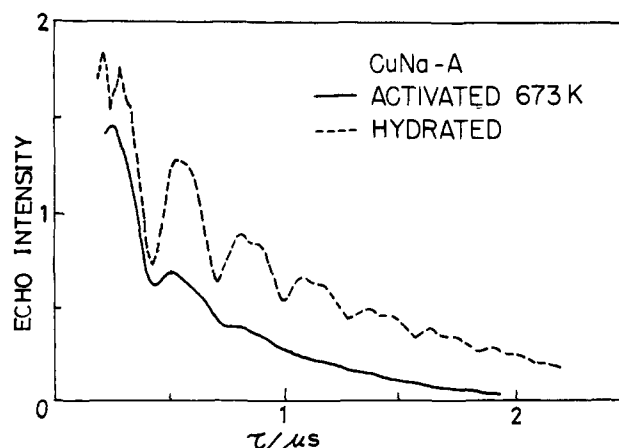


**Figure 3.** Two-pulse electron spin echo signals for  $\text{Cu}^{2+}$  in activated (—) and hydrated (---) Na-A zeolites. The modulation is due to interaction with  $^{27}\text{Al}$  nuclei.

hydrated with  $\text{D}_2\text{O}$  were also the same as those of the initial ones.

Adsorption of methanol on the activated zeolites caused a change in the ESR spectra and modulation patterns. Figure 4 shows the ESR spectra of  $\text{CH}_3\text{OH}$ ,  $\text{CD}_3\text{OH}$ , and  $\text{CH}_3\text{OD}$  adsorbed on CuNa-A zeolite; these should be compared with the ESR spectrum of activated CuNa-A in Figure 1. Although the spectra in Figure 4 show slight differences these are not considered significant. Comparison with Figure 1 shows that the main effect of methanol adsorption is to decrease the sharpness of the hyperfine splittings. In this respect the adsorption of water (see Figure 1) and methanol is similar. As shown in Figure 5, adsorption of  $\text{CH}_3\text{OH}$  causes an increase in the modulation amplitude due to  $^{27}\text{Al}$  as compared to the activated zeolite in Figure 3. In fact, the modulation pattern in Figure 5 is rather similar to the modulation pattern of hydrated CuNa-A zeolite in Figure 3. Figure 6 summarizes the comparison of the  $^{27}\text{Al}$  nuclear modulations for hydrated, methanolated, and activated zeolites more quantitatively by a ratio plot.

Figure 7 shows the experimental and simulated three-pulse modulation patterns for CuNa-A zeolite with adsorbed  $\text{CD}_3\text{OH}$  and  $\text{CH}_3\text{OD}$ . The echo signals are modulated by the deuterium nuclear free precession frequency which is 2 MHz in a 315 mT field. The data were analyzed with use of the ratio analysis described previously. The best fit values of the numbers of surrounding deuterons, the distances between  $\text{Cu}^{2+}$  and D, the isotropic coupling constants, and the decay functions are given in the figure caption. These distances are considered good to  $\pm 0.01$  nm.

In contrast to adsorption of water and methanol, adsorption of ethylene does not change the ESR spectrum of activated

(21) Kevan, L. In "Time Domain Electron Spin Resonance"; Kevan, L.; Schwartz, R. N., Ed.; Wiley-Interscience: New York, 1979; Chapter 8.

(22) Ichikawa, T.; Kevan, L.; Bowman, M. K.; Dikanov, S. A.; Tsvetkov, Yu. D. *J. Chem. Phys.* 1979, 71, 1167.

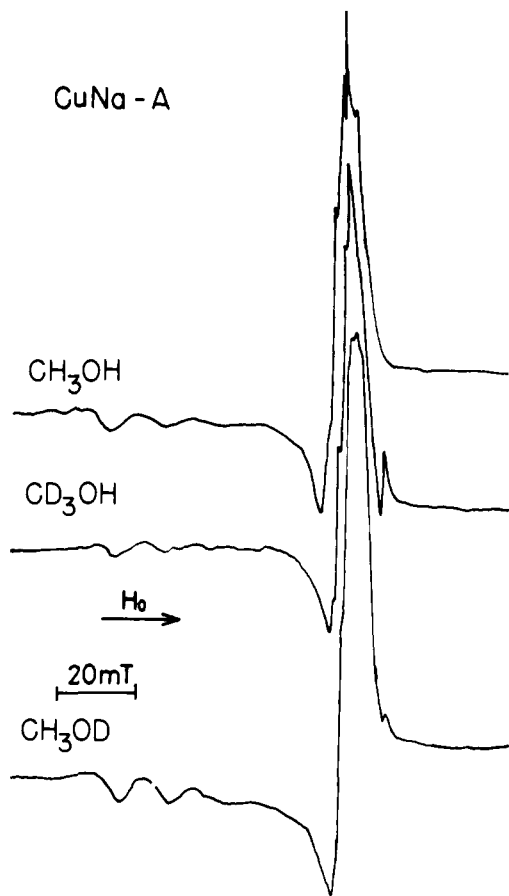


Figure 4. ESR spectra of  $\text{Cu}^{2+}$  in  $\text{CH}_3\text{OH}$ - (upper),  $\text{CD}_3\text{OH}$ - (middle), and  $\text{CH}_3\text{OD}$  (lower)-adsorbed Na-A zeolites.

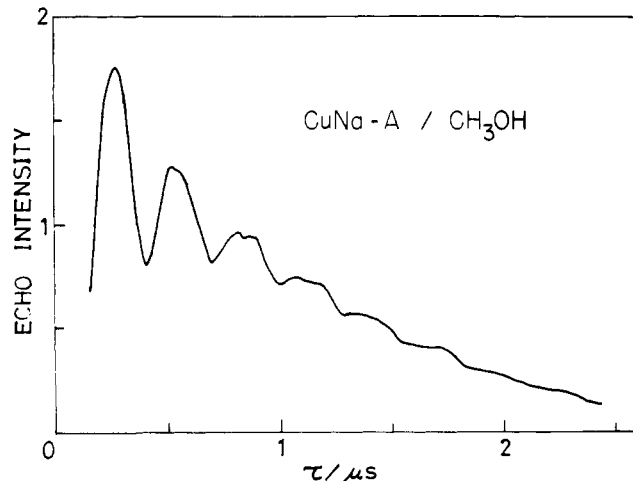


Figure 5. Two-pulse electron spin echo signal for  $\text{Cu}^{2+}$  in Na-A zeolite with adsorbed  $\text{CH}_3\text{OH}$ .

$\text{CuNa-A}$  zeolite much, as shown in Figure 8. This suggests that the adsorption of ethylene is characterized by a much weaker interaction with  $\text{Cu}^{2+}$  than the more polar molecules. Figure 9 shows the two-pulse electron spin echo signal of  $\text{CuNa-A}$  zeolite with adsorbed  $\text{C}_2\text{D}_4$ . Although both  $^{27}\text{Al}$  and  $\text{D}$  nuclei contribute to the modulation, the modulation by  $^{27}\text{Al}$  seems much shallower than that for the hydrated zeolite.

The experimental and simulated three-pulse ESE signals for the  $\text{CuNa-A}$  zeolite with adsorbed  $\text{C}_2\text{D}_4$  are shown in Figure 10. The parameters used for the simulation are given in the figure caption.

#### Discussion

**Movement of  $\text{Cu}^{2+}$  upon Adsorption.** Type A zeolite is composed of  $\text{AlO}_4$  and  $\text{SiO}_4$  tetrahedra bonded together to form truncated

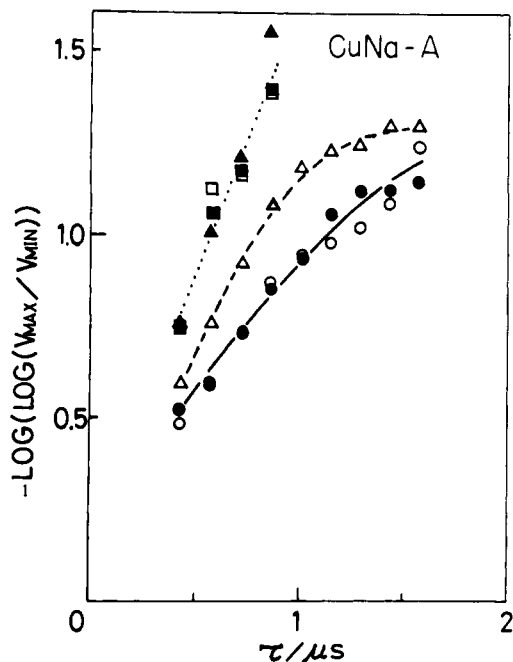


Figure 6. Amplitude of the two-pulse electron spin echo modulation by  $^{27}\text{Al}$  in hydrated  $\text{CuNa-A}$  (O), rehydrated  $\text{CuNa-A}$  (●),  $\text{CuNa-A}$  with adsorbed  $\text{CH}_3\text{OH}$  (Δ), activated  $\text{CuNa-A}$  (□), activated  $\text{CuK-A}$  (■), and activated  $\text{CuCa-A}$  (▲) zeolites.

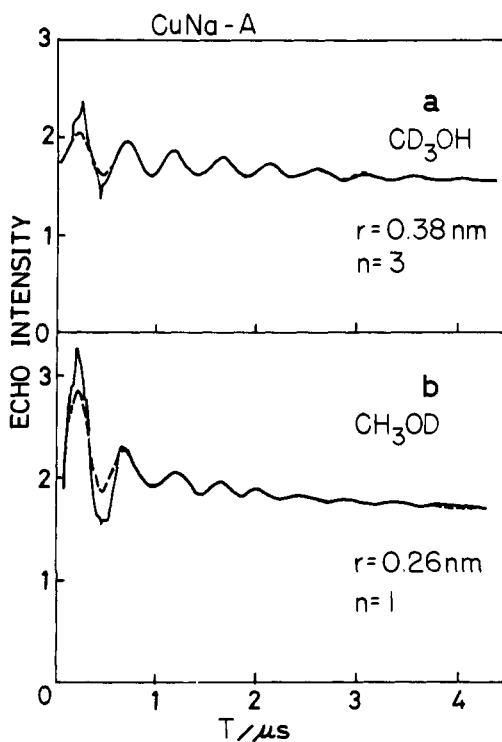
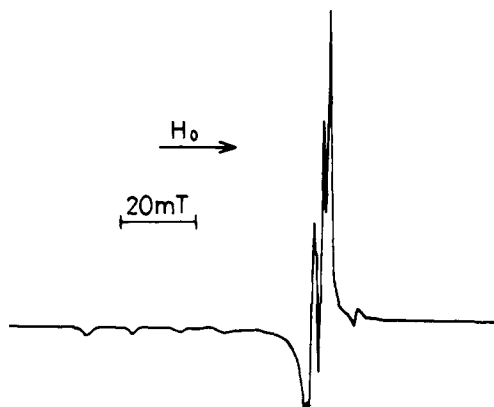
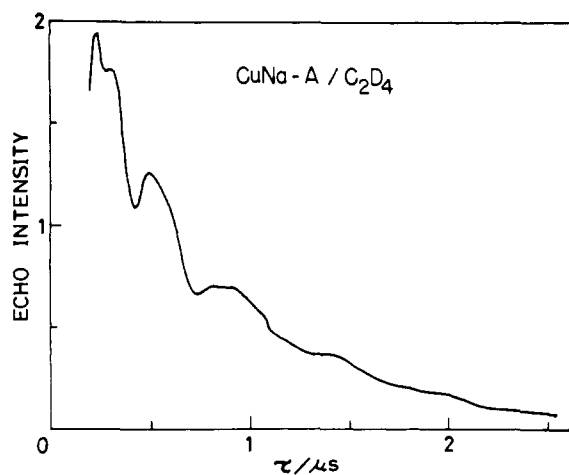
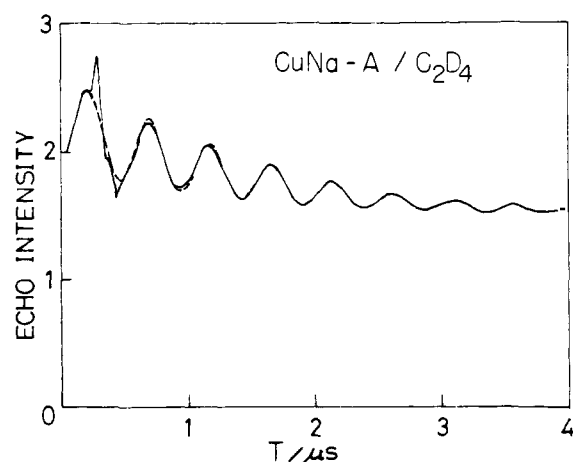


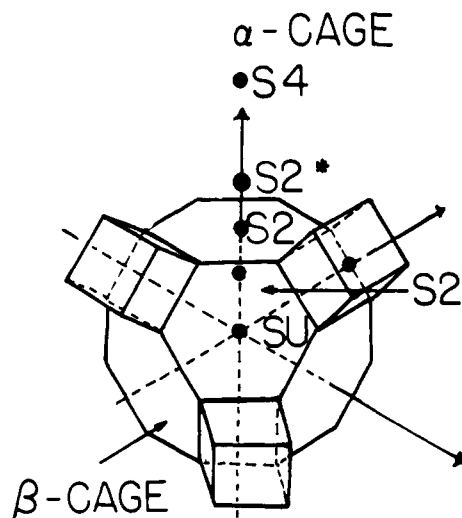
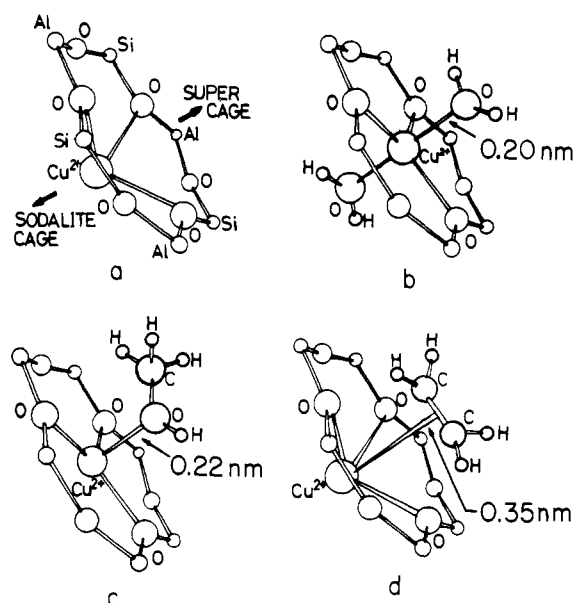
Figure 7. Comparison of the experimental (—) and calculated (---) three-pulse electron spin echo signals for  $\text{Cu}^{2+}$  in  $\text{CD}_3\text{OH}$  (upper) and  $\text{CH}_3\text{OD}$  (lower) methanolated  $\text{CuNa-A}$  zeolites. The parameters used for the calculations are,  $n = 3$ ,  $r = 0.38$  nm,  $a = 0$  MHz and  $g(T) = \exp(0.727 - 0.056T + 0.0024T^2 + 0.00025T^3)$  for  $\text{CD}_3\text{OH}$ , and  $n = 1$ ,  $r = 0.26$  nm,  $a = 0.2$  MHz, and  $g(T) = \exp(1.2 - 0.212T + 0.052T^2 - 0.0049T^3)$  for  $\text{CH}_3\text{OD}$ .

cuboctahedra with eight hexagonal faces and six square faces. These truncated cuboctahedra are called sodalite or  $\beta$  cages and are in turn bonded together by cubes on their square faces to form a larger super cage or  $\alpha$  cage with 26 sides.

Cations are present to compensate for the deficiency of positive charge due to aluminum in the lattice. Various cation sites have been identified by X-ray crystallography.<sup>23-28</sup> The cation sites

CuNa - A / C<sub>2</sub>D<sub>4</sub>Figure 8. ESR spectrum of CuNa-A zeolite with adsorbed C<sub>2</sub>D<sub>4</sub>.Figure 9. Two-pulse electron spin echo signal for Cu<sup>2+</sup> in Na-A zeolite with adsorbed C<sub>2</sub>D<sub>4</sub>.Figure 10. Comparison of the experimental (—) and calculated (---) three-pulse electron spin echo signal for Cu<sup>2+</sup> in Na-A zeolite with adsorbed C<sub>2</sub>D<sub>4</sub>. The parameters used for the calculation are  $r = 0.38$  nm,  $n = 4$ ,  $a = 0$  MHz, and  $g(T) = \exp(0.96 - 0.187T + 0.024T^2 - 0.0002T^3)$ .

of relevance for the current discussion are shown in Figure 11. Site SU is the center of a  $\beta$  cage, site S4 is the center of an  $\alpha$  cage,

Figure 11. View of a  $\beta$  cage in A zeolite showing various cation positions. Site SU is the center of the  $\beta$  cage, site S4 is the center of an  $\alpha$  cage, site S2 is the center of a hexagonal plane or 6-ring between the  $\alpha$  and  $\beta$  cages, and sites S2' and S2\* show displacement along the threefold axis of the 6-ring into the  $\beta$  or  $\alpha$  cages, respectively.Figure 12. Suggested geometries for molecules adsorbed on Cu<sup>2+</sup> in A zeolite: (a) dehydrated or activated; (b) hydrated; (c) adsorbed methanol; and (d) adsorbed ethylene.

and site S2 is the center of a hexagonal face or 6-ring between the  $\alpha$  and  $\beta$  cages. Sites S2' and S2\* correspond to displacements into the  $\beta$  and  $\alpha$  cages, respectively, along the threefold axis through sites SU, S2, and S4.

In a previous ESE study<sup>18</sup> we located Cu<sup>2+</sup> in hydrated A zeolite in site S2 where Cu<sup>2+</sup> is coordinated to two water molecules, one located in the  $\alpha$  cage and one located in the  $\beta$  cage. In this position the Cu<sup>2+</sup> interacts with three Al atoms at 0.31 nm in the 6-ring. Thus the Al modulation pattern in Figure 3 for hydrated CuNa-A is characteristic of this geometry. Changes in this Al modulation pattern upon dehydration or adsorption of molecules other than water indicate movement of Cu<sup>2+</sup> from the S2 site. So the much

(23) Seff, K.; Shoemaker, D. P. *Acta Crystallogr.* 1967, 22, 162.(24) Yanagida, R. Y.; Amaro, A. A.; Seff, K. *J. Phys. Chem.* 1973, 77, 805.(25) Riley, P. E.; Seff, K.; Shoemaker, D. P. *J. Phys. Chem.* 1972, 76, 2593.(26) Yanagida, R. Y.; Vance, T. B., Jr.; Seff, K. *Inorg. Chem.* 1974, 13, 723.(27) Riley, P. E.; Seff, K. *Inorg. Chem.* 1974, 13, 1355.

(28) Breck, D. W. "Zeolite Molecular Sieves"; Wiley-Interscience: New York, 1974.

(29) Ivash, E. V.; Dennison, D. M. *J. Chem. Phys.* 1953, 21, 1804.

reduced Al modulation pattern in the dehydrated sample activated at 673 K indicates that  $\text{Cu}^{2+}$  has increased the  $\text{Cu}^{2+}$ -Al distance and hence has moved away from site S2 upon dehydration. From results with subsequently adsorbed molecules, to be discussed below, we can specify that  $\text{Cu}^{2+}$  moves into the  $\beta$  cage to a site S2' position as shown in Figure 12a. We cannot be certain that  $\text{Cu}^{2+}$  stays on the threefold axis of the 6-ring; it only seems most probable. If this sample is now rehydrated the Al modulation pattern characteristic of site S2 is regained as shown in Figure 6.

If methanol is adsorbed onto activated CuNa-A zeolite, the Al modulation pattern in Figure 5 is obtained. The increased Al modulation depth shows that  $\text{Cu}^{2+}$  has moved from site S2' back toward site S2 in the 6-ring. A quantitative analysis of the Al modulation in Figure 6 shows, however, that the  $\text{Cu}^{2+}$  has not moved all the way back to site S2. The deuterium modulation results, to be discussed below, indicate that  $\text{Cu}^{2+}$  is still about 0.01 nm away from the S2 site position.

If the less polar molecule, ethylene, is adsorbed onto activated CuNa-A zeolite the Al modulation pattern in Figure 9 is obtained. The Al modulation depth has only slightly increased over that of the activated zeolite in Figure 3, showing that  $\text{Cu}^{2+}$  has not moved much back toward site S2.

This set of experiments shows a clear correlation between the position of  $\text{Cu}^{2+}$  and the polarity of the adsorbate molecules. Now we examine the geometry of the adsorbate molecules around  $\text{Cu}^{2+}$ .

**Geometry of Adsorbate Molecules.** Figure 12b shows the adsorbate geometry of hydrated<sup>18</sup> or rehydrated CuNa-A zeolite. Two water molecules are coordinated to  $\text{Cu}^{2+}$ , one in the  $\alpha$  cage and one in the  $\beta$  cage. The water dipole directions are oriented toward  $\text{Cu}^{2+}$  and the  $\text{Cu}^{2+}$  to  $\text{O}(\text{H}_2\text{O})$  distance is 0.20 nm. The adsorbate geometry of rehydrated zeolites is identical with that of originally hydrated zeolite.

Figure 7 shows the deuterium modulation patterns for adsorbed  $\text{CD}_3\text{OH}$  and  $\text{CH}_3\text{OD}$ . In both cases the number of equivalent interacting deuterons around  $\text{Cu}^{2+}$  is indicative of only one coordinated methanol molecule. Methanol is too large to enter the  $\beta$  cage so the one methanol coordinated to  $\text{Cu}^{2+}$  must be in the  $\alpha$  cage. This allows us to determine that  $\text{Cu}^{2+}$  in the activated zeolite must be in a site S2' position rather than an S2\* position (see Figure 11). Coordinated methanol in the  $\alpha$  cage can pull  $\text{Cu}^{2+}$  from an S2' toward an S2 position and increase the Al modulation depth as observed while if  $\text{Cu}^{2+}$  had been in an S2\* position methanol coordination would have pulled  $\text{Cu}^{2+}$  still further away from the 6-ring and would have decreased the Al modulation depth.

The orientation of the adsorbed methanol relative to  $\text{Cu}^{2+}$  is determined from the distances to the  $\text{CD}_3$  and  $\text{OD}$  deuterons. From the experimental distances given in Figure 7 and the known geometry of methanol the orientation shown in Figure 12c is deduced. The average distance from  $\text{Cu}^{2+}$  to the methyl deuterons is calculated from a locked configuration of the methyl group averaged over  $360^\circ$  about the C-O axis. From Figure 12c it can be seen that the bisector of the COH bond angle of methanol is oriented toward the  $\text{Cu}^{2+}$ . The molecular dipole of methanol is also approximately oriented along this angle bisector<sup>29</sup> so the adsorbate structure seems to be controlled by a cation charge-molecular dipole interaction. This is the same as deduced for water adsorbate.

The orientation of ethylene adsorbate is determined from the deuterium modulation in Figure 10. The interaction with four equivalent deuterons at 0.38 nm indicates only one ethylene adsorbate molecule with its molecular plane perpendicular to a line toward  $\text{Cu}^{2+}$ ; this geometry is portrayed in Figure 12d. From the known geometry of ethylene the distance from the  $\text{Cu}^{2+}$  to the center of the C=C double bond is deduced to be 0.35 nm. Ethylene is too large to enter the  $\beta$  cage and the geometry shown in Figure 12d implies a rather weak interaction with  $\text{Cu}^{2+}$ . However, this geometry does appear to maximize the cation charge-molecular polarizability interaction since the double bond is the most polarizable region of ethylene. Thus, this interaction is likely the controlling one for the ethylene adsorbate geometry

in A zeolite.

**Location of the S2' Site.** The S2' site of  $\text{Cu}^{2+}$  in activated A zeolite has not been quantitatively located in terms of its distance from the S2 site in the 6-ring because we cannot quantitatively analyze the Al modulation. Here we attempt to locate this S2' site from the molecular adsorbate geometries. In hydrated A zeolite a  $\text{Cu}^{2+}$ - $\text{O}(\text{H}_2\text{O})$  distance of 0.20 nm was obtained.<sup>18</sup> This fits the sum of the cupric ion radius of 0.07 nm and the 0.14 nm covalent radius of an oxygen atom.<sup>30</sup> For adsorbed methanol we obtain a  $\text{Cu}^{2+}$ - $\text{O}(\text{CH}_3\text{OH})$  distance of 0.22 nm. If  $\text{Cu}^{2+}$  remained in the same position as with adsorbed water we would expect the same  $\text{Cu}^{2+}$ -O distance, given the orientations of water and methanol, toward  $\text{Cu}^{2+}$ . Thus the 0.22 nm distance suggests that  $\text{Cu}^{2+}$  is displaced 0.02 nm away from site S2 in the 6-ring into the  $\beta$  cage. This is supported by the fact that we obtain a  $\text{Cu}^{2+}$ -O distance of 0.21 nm for  $\text{Cu}^{2+}$  solvation in bulk methanol.<sup>31</sup> Of course, this small distance change is within our experimental fitting error, but the Al modulation with adsorbed water and methanol clearly supports a distance change of this size or perhaps greater.

Now consider the case of adsorbed ethylene where we obtain a distance of 0.35 nm from  $\text{Cu}^{2+}$  to the molecular plane of ethylene and where the Al modulation indicates that  $\text{Cu}^{2+}$  is still close to the S2' site in activated A zeolite. To determine the  $\text{Cu}^{2+}$  displacement from the S2 site we must estimate how far the ethylene plane is from the 6-ring. The ethylene plane has a half thickness of 0.17 nm due to its  $\pi$  bonds.<sup>30</sup> To this we will add 0.07 nm as a maximum effective half thickness of the 6-ring. This is the same as if  $\text{Cu}^{2+}$  were in site S2; it is possible that ethylene may be able to approach even closer when the  $\text{Cu}^{2+}$  is displaced. This leaves  $0.35 - 0.17 - 0.07 = 0.11$  nm as the displacement of the  $\text{Cu}^{2+}$  from the S2 site. The Al modulation indicates that this displacement is slightly greater, probably by 0.01 to 0.02 nm based on the water-methanol comparison of Al modulation. Thus we assign site S2' in activated A zeolite to be  $0.12 \pm 0.02$  nm from site S2.

**Comparison of ESR Spectra with Adsorbate Geometry.** The ESR spectra of hydrated CuNa-A zeolite change markedly upon activation. As shown in Figure 1 the copper hyperfine splitting becomes much sharper and better resolved in the  $g_{\perp}$  region. The sharpness of these splittings is largely lost upon rehydration or adsorption of methanol. On the other hand, adsorption of ethylene does not affect the sharpness or resolution appreciably. From the adsorbate geometries we have deduced in Figure 12 it is evident that the position of  $\text{Cu}^{2+}$  relative to a 6-ring between the  $\alpha$  and  $\beta$  cages is correlated with the appearance of the ESR spectra. When  $\text{Cu}^{2+}$  is in site S2 or within  $\sim 0.02$  nm from there the  $g_{\perp}$  hyperfine resolution is poor. But when  $\text{Cu}^{2+}$  is in site S2', which is  $\sim 0.12$  nm from S2, the  $g_{\perp}$  hyperfine components are much sharper with improved resolution. The difference is perhaps related to unresolved hyperfine with  $^{27}\text{Al}$  nuclear spins and with H or D nuclear spins on the adsorbate molecules. At any rate the ESR spectra themselves are somewhat diagnostic of the cation position, now that we have elucidated the adsorbate geometry.

## Conclusions

The location of  $\text{Cu}^{2+}$  in the A zeolite framework is a rather sensitive function of the  $\text{Cu}^{2+}$ -adsorbate interactions. Variations of the  $\text{Cu}^{2+}$  distance in the  $\beta$  cage from the hexagonal face between the  $\alpha$  and  $\beta$  cages in the zeolite structure can be varied up to about 0.14 nm by selection of the adsorbate. Stronger adsorbates in the  $\alpha$  cage pull  $\text{Cu}^{2+}$  toward the hexagonal face while weaker adsorbates leave  $\text{Cu}^{2+}$  displaced further into the  $\beta$  cage. This manipulation of the  $\text{Cu}^{2+}$  position in slightly exchanged A zeolite is in considerable contrast to  $\text{Mn}^{2+}$  in  $\text{Mn}_{4.5}\text{Na}_3\text{-A}$  which shows little change in position with various adsorbates.<sup>32,33</sup>

**Acknowledgment.** This research was supported by the National Science Foundation.

(30) Pauling, L. "Nature of the Chemical Bond", 3rd ed.; Cornell University Press: Ithaca, New York, 1960; pp. 260, 514, and 518.

(31) Ichikawa, T.; Kevan, L. *J. Phys. Chem.* **1980**, *84*, 1955.

(32) Riley, P. E.; Seff, K. *Inorg. Chem.* **1975**, *14*, 715.

(33) Seff, K. *Acc. Chem. Res.* **1976**, *9*, 121.